CREEP CRACK GROWTH BEHAVIOUR OF ALLOY 718

C.D. Liu, Y.F. Han, M.G. Yan and M.C. Chaturvedi*

Institute of Aeronautical Materials, Beijing China, 100095

*Department of Mechanical Engineering, The University of Manitoba
Winnipeg, Manitoba, Canada R3T 2N2

ABSTRACT

The creep crack growth behaviour of Alloy 718 at 923K has been investigated. It is found that its creep crack growth is controlled by stress intensity factor regardless of load level, loading change and crack growing history. The metallographic analysis indicates that the creep crack growth mechanism of this alloy at 923K comprises three stages. Based on this mechanism, a creep crack growth model has been developed where crack growth rates relate with the effective driving force in sinh function. In addition, the effect of microstructure on the creep crack growth behaviour of Alloy 718 has been studied. The results reveal that the crack growth rates strongly depend on the grain size and the carbide structure. These phenomena have been explained by the diffusion and tearing process in the creep crack growth mechanism.

Superalloys 718, 625 and Various Derivatives
Edited by Edward A. Loria
The Minerals, Metals & Materials Society, 1991

INTRODUCTION

With the progress of technology, hot section components such as turbine discs and blades in jet engines are being used at higher and higher temperatures which has a tendency to reduce the useful life of the parts. To improve the reliability and durability of gas engines, the Engine Structure Integrity Program (ENSIP) has been developed for their design. With the evolution of structure integrity, damage tolerance design has been recommended for critical components. Since creep is an important factor in causing the hot section components of gas engines to fail, it is necessary to study the creep crack growth behaviour of materials used at elevated temperatures.

Since Thornton (1) studied creep crack growth with single edge specimens in 1972, many investigations have been carried out to seek a characterizing parameter. The creep crack growth being an inelastic process, net section stress σ_n (2) and reference stress σ_r (3) have been used to correlate with creep crack growth rates. In 1976, based on the modification of the J integral, a C* integral was suggested to be an appropriate parameter for creep crack growth (4-7). However, the C* integral represents only the amplitude of the stress strain field ahead of the crack tip when a material is in steady state creep, but the stress relaxation around the crack tip due to creep deformation and crack propagation causes a nonsteady state creep process. This imposes many limitations on the use of the C* integral. Recently, a creep integral (13) has been developed to describe nonsteady state creep crack growth (14) which is suggested to successfully characterize nonsteady state creep crack growth behaviour. The stress intensity factor has also been suggested to be an appropriate parameter for creep crack growth measurements (15, 16). Since the stress intensity factor results from linear elastic fracture mechanics, there is always doubt as to whether it can be used to describe creep crack growth, although the stress intensity factor is much better than other parameters for correlating with creep crack growth rates of some materials (17). In a previous study (18), the condition under which the stress intensity factor can be used as a parameter for creep crack growth was analyzed. It was found that the stress intensity factor would be a single parameter to characterize creep crack growth. This investigation focuses on the creep crack growth behaviour of Alloy 718 at 923K and includes a creep crack growth law, a creep crack growth mechanism, as well as the effect of microstructure on creep crack growth behaviour.

Material and Experimental Techniques

The material used in the present investigation was Alloy 718. The as-received material was a 90x90 mm bar of the following chemical composition.

Table 1. Chemical Composition of Alloy 718

Ni	Cr	Mo	Nb	Al	Ti	Fe	Mn	Si	C
1.8	18.9	3.06	5.04	0.56	0.9	19.4	0.1	0.65	0.035

Standard compact tension specimens with a width of W=40 mm and a thickness of B=20 mm were used in this study. The heat treatment given to the specimens was 1238K/1/AC +993K/8/FC+893K/18/AC. The 10mm long cracks in the CT specimen were cut with an electric line cutting machine. 2mm long fatigue cracks were introduced in an universal 1256 Instron machine at room temperature under a stress intensity factor of 895 MPa $\sqrt{mm}$ with a load ratio R=0.1. The creep crack growth tests were carried out in a DST-5 constant load creep machine at a temperature of 923K. The testing temperature was controlled within $\mp$2K using a three-zone furnace. The crack opening displacement was measured by a LVDT through an extensometer. The accuracy of the LVDT was 0.002 mm. The crack lengths were measured by the elastic compliance method.

Characteristic Parameter

It is important to define a characterizing parameter in creep crack growth. For stainless steel (8-12), the C* integral has been successfully correlated with creep crack growth rates. In some investigations (1, 2, 15-17), the stress intensity factor has also been used to correlate with the creep crack growth data, but not convincingly. For a steady crack, a limiting creep zone has been defined based on the conception of limiting creep. In this case, the stress intensity factor is expressed as (18)

$$\text{Min } \{a, W\text{-}a\} > 0.5 \left(\frac{K^2}{\sigma_n}\right) \qquad (1)$$

and can be used as a governing parameter for creep crack growth. In this expression, σ_n is the creep limit which for Alloy 718 was observed to be 491 MPa at 923K (19). By substituting this value into inequality (1), it is found that the stress intensity factor will be a valid parameter to represent stress strain fields ahead of the crack tip during the creep crack growth of Alloy 718 when applied loads are in the range of 12252 to 19635 N.

The compliance in the creep crack growth test of Alloy 718 has been measured. The results show that the difference between elastic compliance and the total compliance is within 10%, which indicates that elastic deformation is predominant throughout the creep crack growth of this alloy.

To study creep crack growth behaviour of alloy 178, different types of creep crack growth tests have been designed and conducted. The creep crack growth rates have been plotted with stress intensity factors as shown in Fig. 1. It has been found that the creep crack growth rates under different loads is almost identical when they are in the same stress intensity factor and loading

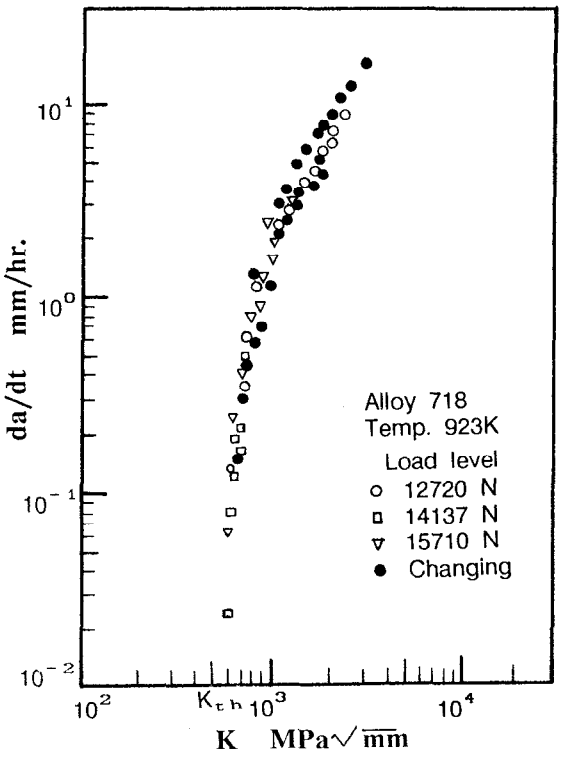

Figure 1. Stress intensity factor as a characterizing parameter for creep crack growth of Alloy 718 at 923K.

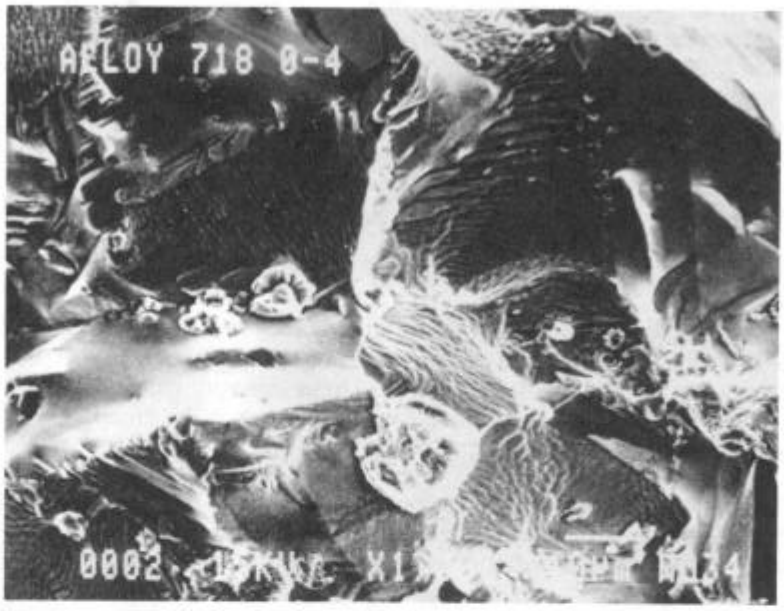

Figure 3. SEM fractograph features shows connection of main crack with new microcrack by tearing in creep crack growth of Alloy 718 at 923K.

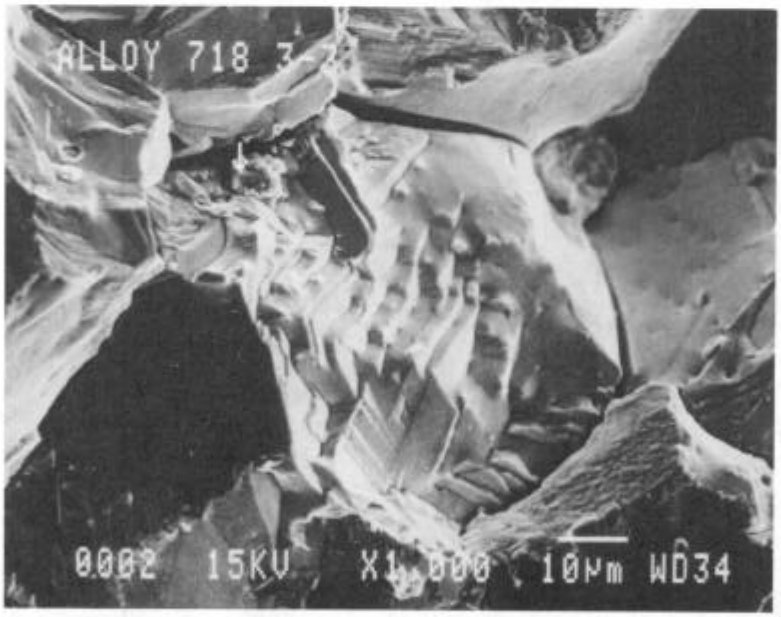

Figure 4. Cleavage cracking features observed by SEM in the creep crack growth of Alloy 718 at 923K.

In general, if the new microcrack initiated from dislocation glide and twinning, it would result in many undulations on the fracture surface even during intergranular cracking. However, in the present investigation a smooth fracture surface has been observed, as shown in Fig. 3. This indicates that this area is caused by vacancy diffusion and segregation in the grain boundary.

change history does not affect the dependence of creep crack growth rates on stress intensity factor. It indicates that the creep crack growth of Alloy 718 at 923K can be characterized by the stress intensity factor. From Fig. 1, it can be seen that the creep crack growth rates approach zero as the stress intensity factor approaches K_{th}. That is, a creep crack growth threshold exists in Alloy 718 at 923K.

Creep Crack Growth Mechanism

In order to investigate the creep crack growth mechanism, a sample containing the crack tip after the crack had propagated 10mm was cut from a creep crack growth specimen and was used for microstructural analysis. Before microstructural observation, the sample was etched in a solution of $5mlHNO_3+30mlH_2O$.

The microstructural observations were made on a surface of the middle thickness section of a specimen. Fig. 2 shows the growing creep crack tip. It can be observed that an intergranular microcrack has initiated at a distance of one to three grains away from the main crack tip. The main crack and the new microcrack are indicated by arrows A and B respectively. This indicates that creep crack growth in Alloy 718 at 923K is a discontinuous process.

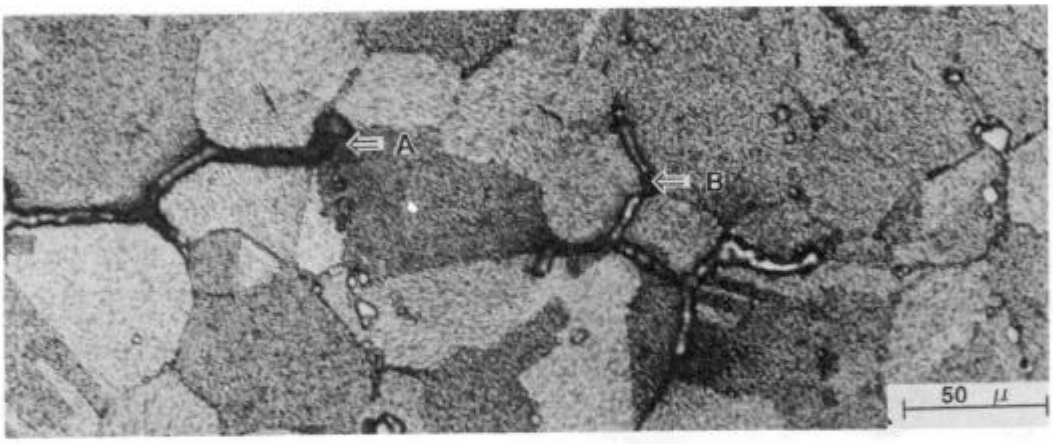

Figure 2. Optical micrograph showing a creep crack tip in Alloy 718 specimen tested at 923K.

The fracture surface of a creep crack was observed by using a JEOL 840 scanning electron microscope. The SEM fractograph of a creep crack in alloy 718 as shown in Fig. 3 reveals that creep cracking is a mixture of intergranular and transgranular cracks. The fracture surface in the left and right regions of the picture is intergranular and that in the middle region has a river-like pattern which is caused by tearing. This fractograph is in good correspondence with the optical picture of the creep crack tip shown in Fig. 2. The intergranular area in the left and right regions of the picture corresponds to the main crack and the new microcrack, respectively. The middle area in this picture indicates that the main crack and the new microcrack are connected by the tearing process. In some areas, the cleavage fracture characteristics have also been observed, as shown in Fig. 3. This suggests that linkage of the main crack and the microcrack is due to cleavage in the facet of the crystal. The particles which seem to be the cause of the initiation of the tearing and cleavage process can be seen in Figs. 3 and 4. It appears that the river-like pattern initiates from particles containing 57% Nb. It is likely that they are niobium carbide particles, although the carbon content of the particles could not be determined by the EDS technique.

From the above SEM fractograph it may be proposed that the creep crack growth of alloy 718 can be divided into three stages.

1) Microcrack initiation stage: for a creep cracked specimen, the stress will concentrate at the triple grain boundary point ahead of the creep crack tip leading to a local increase in strain energy. Since vacancies diffuse from a low strain energy position to a high energy position, many vacancies will segregate at the triple grain boundary point by diffusion which gives rise to new microcracks.

2), Microcrack growth stage: After a microcrack initiation, the stress will be largely concentrated at the microcrack tip, and vacancies will more quickly diffuse to the microcrack tip along the grain boundary, leading to the growth of the microcrack with time. For a specimen crept at intermediate temperature, the velocity of the vacancy diffusion along the surface is much lower than that along the grain boundary, i.e., $Vs << Vg$. The creep crack growth is controlled by the vacancy diffusion along grain boundaries. Therefore, the vacancy diffusion will form cracks rather than cavities.

3) Linkage stage: As the new crack grows, the local J integral or stress intensity factor K increases. Once the value of the local J integral at the new crack tip or the main crack tip reaches the fracture toughness Jic of the material, an unstable fracture will start from the new crack tip or the main crack tip, to break the ligament between the two cracks, i.e., the main crack and the microcrack will join each other, leading to creep crack growth.

Therefore, the creep crack growth of Alloy 718 at 923K is due to the vacancy diffusion and tearing process; that is,

$$\frac{da}{dt} = \frac{\Delta a_{d+} \Delta a_t}{\Delta t} \qquad (2)$$

Three assumptions are made in establishing the creep crack growth model:

1). The new microcrack initiates at a characteristic distance, rc, from the main crack tip. This distance relates to the stress intensity factor.

2). Microcrack growth caused by the vacancy concentration is governed by thermally activated vacancy diffusion which is a thermodynamic process.

3). The crack length increment in the tearing process is proportional to the driving force, G.

From these three assumptions, it has been deduced that the creep crack growth in Alloy 718 at 923K can be represented by the effective driving force, G_e, as (18).

$$\frac{da}{dt} = \eta \frac{D_{gb}}{d} \text{sh} \left[\frac{cG_e}{kT}\right] \qquad (3)$$

where $G_e = (K^2 - K^2_{th})/E$ and K_{th} is the threshold stress intensity factor for creep crack growth, D_{gb} is the diffusion coefficient in the grain boundary material, d is the grain size and η is a material constant associated with the material surface energy.

Effect of Grain Size on Creep Crack Growth

In order to investigate the effect of grain size on creep crack growth behaviour, creep crack growth tests were performed on the specimens with two different grain sizes as shown in Fig. 5.

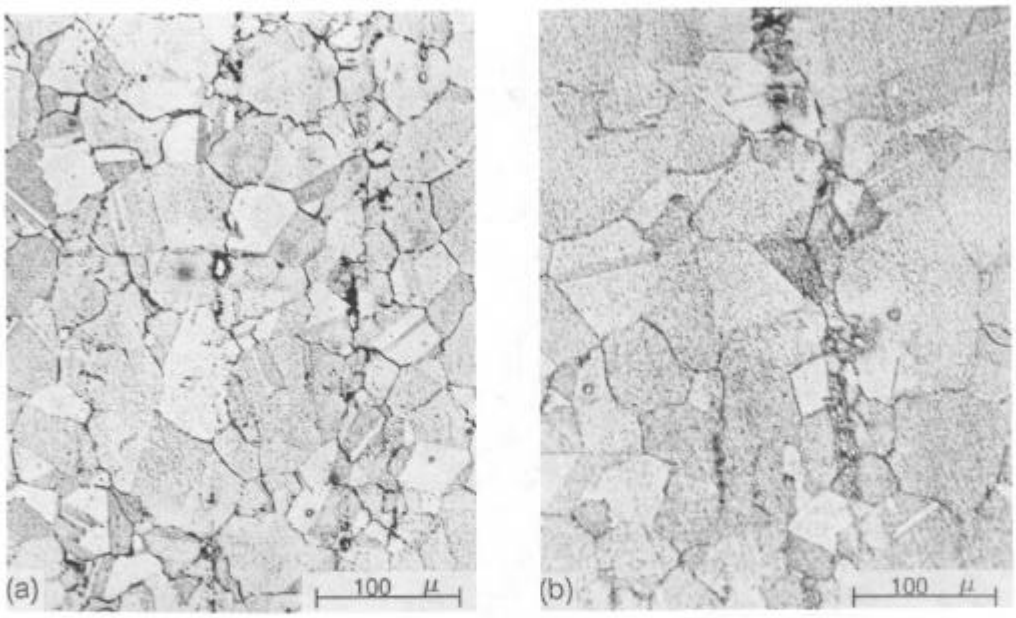

Figure 5. Difference of grain size in two specimens of Alloy 718 (a) 40μm (b) 65μm

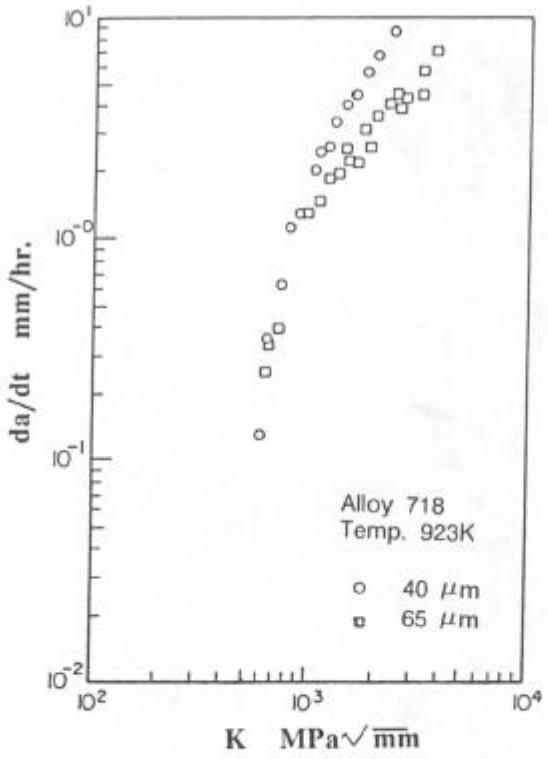

Figure 6. Grain size effect on creep crack growth in Alloy 718 at 923K

The test results are shown in Fig. 6, where crack growth rates are plotted with stress intensity factor. It is observed that the creep crack growth rates are affected by the grain size and this effect is enhanced as the stress intensity factor increases. However, as the stress intensity factor approaches the threshold, the grain size does not effect the creep crack growth rates.

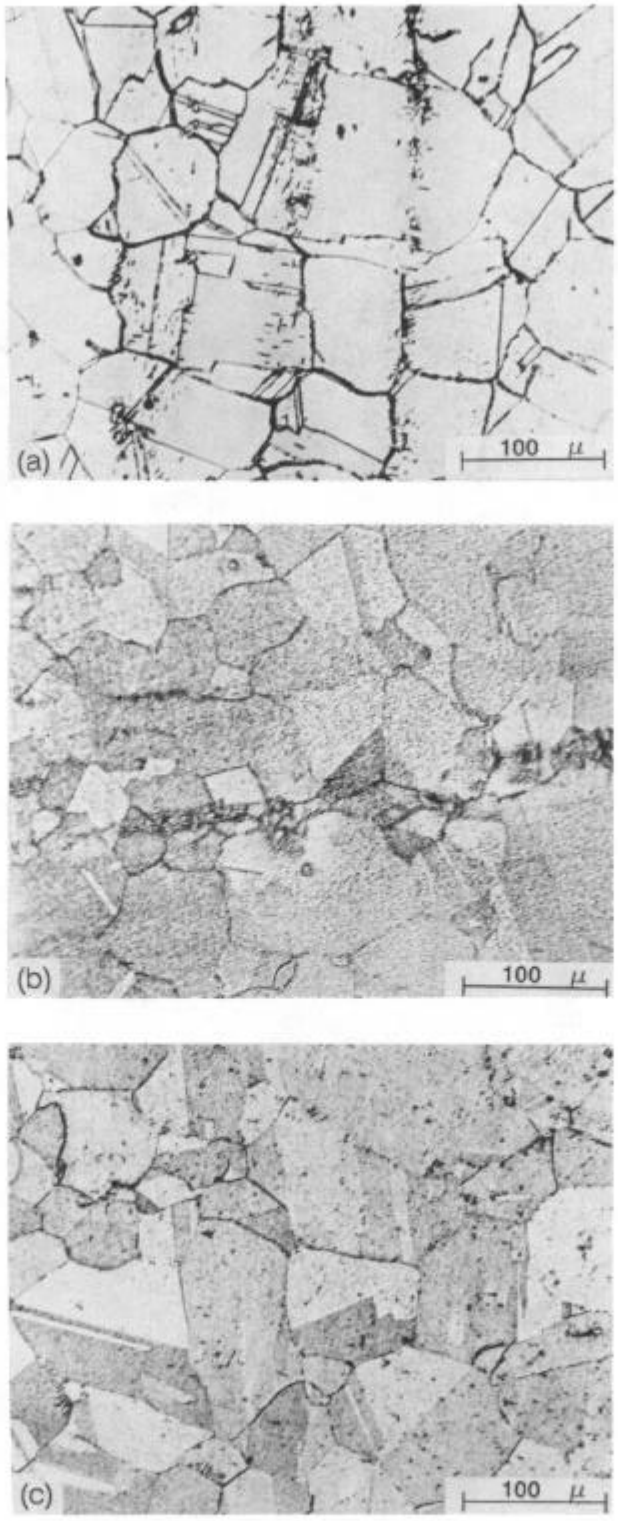

Figure 7. Three kinds of carbides structure in Alloy 718
(a) Carbides parallel to the crack
(b) Carbides perpendicular to the crack
(c) Carbides homogeneously distributed

That is, the grain size does not influence the creep crack growth threshold of Alloy 718 at 923K.

The phenomena of the influence of grain size on the creep crack rate can be interpreted by the creep crack growth mechanism suggested in the previous section. According to diffusion theory, larger the grain size, the longer the diffusion path. Therefore, the specimen with larger grain size will need more time for crack initiation and growth. Therefore, the creep crack growth rates must be inversely proportional to grain size as expressed in equation (3). The test results shown in Fig. 6 reveal that the creep crack growth rate of a specimen with a 40μm grain size is about 1.5 times larger than that observed in a specimen with 65μm grain size. This is in agreement with the creep crack growth mechanism model.

Effect of Carbides Structure on Creep Crack Growth

Three specimens with different carbide distribution were used to investigate the role of carbides in creep crack growth behaviour. In one, the carbides were parallel to the crack direction; in another, the carbides were perpendicular to the crack direction, and in the third specimen, fine carbides were homogeneously distributed in grain boundaries and inside grains, as shown in Fig. 7. The grain sizes of the three specimens were slightly different, i.e., 68, 65 and 71 μm respectively. Since the stress intensity factor is the controlling parameter in the creep crack growth of Alloy 718 at 923K, the creep crack growth rates for the three kinds of specimen have been plotted against stress intensity factor in Fig. 8. These results show that the material with homogeneous fine carbides has the lowest creep crack growth rates and the best resistance to creep crack growth, and the specimen with carbides perpendicular to the crack exhibits much lower creep crack growth rate than the one with carbides parallel to the crack. This means that carbide distribution affects the creep crack growth of Alloy 718 tested at 923K.

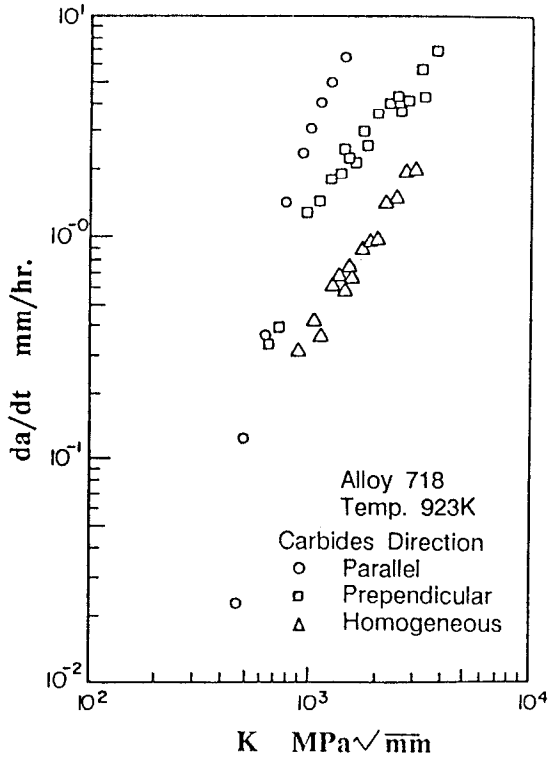

Figure 8. Effect of Carbide distribution on creep crack growth of Alloy 718 at 923K

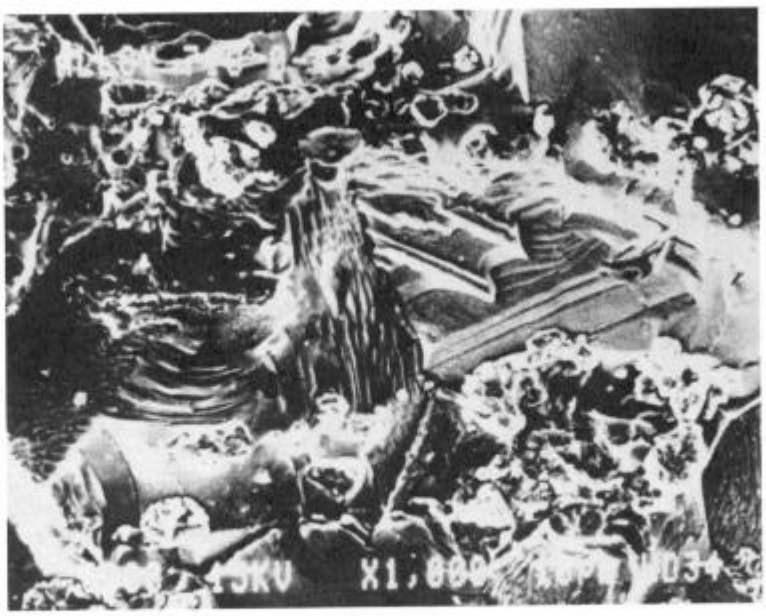

Figure 9. SEM fractograph showing cleavage features and carbides on fracture surface in specimen with carbides parallel to the crack after creep crack growth in Alloy 718 at 923K.

Figs 9 and 10 are the SEM fractographs of specimens after creep crack growth in specimens with two different carbide distributions. It can be seen that there is a significant difference between them. For the specimen with carbides parallel to the crack direction, a lot of carbides are seen in Fig. 9. However, in Fig. 10, the specimen with homogeneously fine carbides, very few carbides are present on the fracture surface which consists of tearing and an intergranular cracking region.

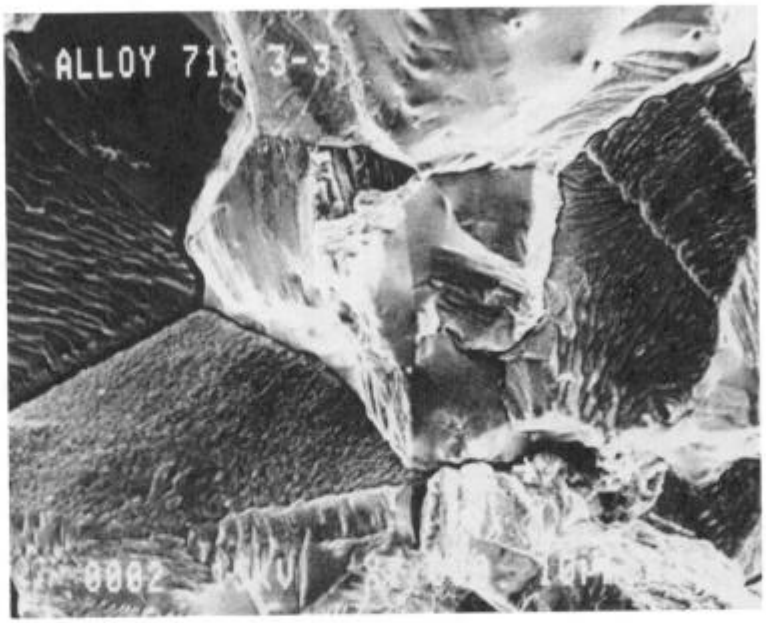

Figure 10. SEM fractograph showing tearing features in specimen with homogeneously distributed fine carbides after creep crack growth in Alloy 718 at 923K.

The creep crack growth mechanism discussed above suggests that the creep crack growth of Alloy 718 at 923K can be divided into three stages. The crack length increment is composed of two parts; one is contributed from vacancy diffusion, whereas the other is due to the tearing process which links new microcracks with the main crack. In Figs. 9 and 10, it has been observed that the tearing or cleavage initiates from the carbides. Hence, carbide distribution affects the creep crack growth through the tearing process. Aligning carbides would considerably reduce local fracture toughness through the tearing process and would considerably reduce local fracture toughness to advance tearing or cleavage. As a result, it would reduce the ligament and the time for new microcrack growth. Therefore, it accelerates crack propagation, especially for the case of carbide induced cleavage.

Conclusions

1. The stress intensity factor is an appropriate parameter to represent the creep crack growth behaviour of Alloy 718 at 923K. Load level, loading change and crack growth history do not seem to affect the dependence of creep crack growth rate on the stress intensity factor.

2. The creep crack growth mechanism of Alloy 718 at 923K consists of three stages: 1) microcrack initiation stage, 2) microcrack growth stage, 3) linkage stage.

3. The creep crack growth law of Alloy 718 at 923K can be expressed as follows

$$\frac{da}{dt} = \eta \frac{D_{gb}}{d} \sinh\left[\frac{cG_e}{kT}\right]$$

Vacancy diffusion in the grain boundary and local fracture toughness determined by the material microstructure play an important role in this creep crack growth law.

4. Grain size affects the creep crack growth behaviour of Alloy 718 at 923K. This effect mainly relates to the diffusion process. The larger grain size has the longer diffusion path leading to the postponement of the time for microcrack initiation and a reduction in the microcrack growth rates.

5. Carbide distribution influences creep crack growth behaviour significantly, since the carbide distribution determines the local fracture toughness. The carbide distribution affects the creep crack growth behaviour of Alloy 718 at 923K via the tearing process.

References

1. Thornton, D.V., "Creep Crack Growth Characteristics of Ferritic Steel:, Conf. on Properties of Creep Resistant Steels, Paper 6.5 (Verein Deutuscher Eisenhutteneute, Dusseldorf, Germany)(1972).

2. Harrisson, C.B. and Sandor, G.N., "High Temperature Crack Growth in Low Cycle Fatigue", Eng. Frac. Mech., Vol. 3, pp 403-420 (1971).

3. Nicholson, R.D., and Formby, C.L., "The Validity of Various Fracture Mechanics Methods at Creep Temperatures:, Int. J. Fracture, Vol. 11, pp 595-604 (1975).

4. Turner, C.E. and Webater, G.A., "Application of Fracture Mechanics to Creep Crack Growth", Int. J. Fracture (10), pp 455-458, (1974).

5. Landes, J.D., and Begley, J.A., "A Fracture Mechanics Approach to Creep Crack Growth", Mechanics of Crack Growth, ASTM STP60l, pp 128-148, (1976)

6. Nikbin, K.M., Webster, G.B. and Turner, C.E., "Relevance of Nonlinear Fracture Mechanics to Creep Cracking", Cracks and Fracture ASTM STP601, pp. 47-62, (1976).

7. Riedel, H. and Rice, J.R., "Tensile Cracks in Creeping Solids", 12th National Symp. on Fracture Mechanics, ASTM STP700, pp. 112-130, (1980).

8. Koterazawa, R. and Mori, T., "Applicability of Fracture Mechanics Parameters to Crack Propagation under Creep Condition", J. Eng. Mater. and Tech., Trans. of ASEM, Vol 99, pp. 298-305, October. (1977).

9. Taira, S., Ohtani, R. and Kitamura, "Application of J Integral to High Temperature Charck Propagation, Part 1-Creep Crack Propagation", T.J. Eng. Mater. and Tech., Trans of ASME, Vol 101, pp 154-161, April (1979).

10. Harper, M.P. and Ellison, E.G., "The Use of the C* Parameter in Predicting Creep Crack Propagation Rates", J. Strain Analysis, Vol 12, pp 167-177, (1977).

11. Christian, E.M. et al., "Critical Examination of Parameters for Predicting Creep Crack Growth", Advances in Fracture Research, ICF-5, Cannes, France, pp. 1295-1303, (1980).

12. Nikbin, K.M. and Webster, G.A., "Temperature Dependence of Creep Crack Growth in Aluminum Alloy RR58", Micro and Macromechanics of Crack Growth, edited by K. Sadananda et al., The Metall. Society of AIME, pp. 137-147, (1981).

13. Atluri, S.M., "Path-independent Integral in Finite Elastisity and Inelastisity, with Body Force Inertia and Arbitary Crack Face Conditions", Eng. Frac. Mech., Vol. 16, pp. 341-369, (1982).

14. Liu, C.D., Han, Y.F. and Yan, M.G., "Nonsteady Creep Crack Growth", submitted to Eng. Frac. Mech., (1990).

15. Siverns, M.J. and Price, A.T., "Crack Propagation Under Creep Conditions in a Quenched 2 1/4 Cr Mo Steel", Int. J. of Fracture, Vol. 9, No. 2, pp. 199-208, (1973).

16. Floreen, S., "The Creep Fracture of Wrought Nickel-base Alloys by a Fracture Mechanics Approach", Metall. Trans. 6A , pp. 1741-1749, (1975).

17. Donath, R.C., Nicholson, T. and Fu, L.S., "An Experimental Investigation of Creep Crack Growth in In100", 13th National Conf. on Fracture Mechanics, ASTM STP743, pp. 186-206, (1981).

18. Liu, C.D., Han, Y.F., Yan, M.G. and Chaturvedi, M.C., "Small Scale Creep Crack Growth", submitted to Eng. Frac. Mech., (1990).

19. Liu, C.D., Han, Y.F. and Yan, M.G., "A New Creep Constitutive Model of Dislocation Thermal Activation", In 19th Canadian Fracture Conference on "Constitutive Law of Plastic Deformation and Fracture, edited by A.S. Krausz et al, Kluwer Academic Publisher, Printed in the Netherlands, pp. 181-187, (1990).